Explor Anim Med Res,
Vol.12, Issue - 1, 2022, p. 109-117
DOI : 10.52635/eamr/12.1.109-117

ISSN 2277- 470X (Print), ISSN 2319-247X (Online)
Website: www.animalmedicalresearch.org

Research Article

DESIGN AND ANALYSIS OF AN EFFICIENT GLAUCOMA MODEL FOR EVALUATION OF PHARMACOLOGICAL TRIALS

Gabriela Aylén Caballero[1], Natalia Angel Villegas[2], David César Cremonezzi[3], Vilma Reneé Campana[1,4], Santiago Daniel Palma[2], Daniel Allemandi[2], Luis Ignacio Tártara[1,2 *]

Received 18 June 2021, revised 14 April 2022

ABSTRACT: Glaucoma is a multifactorial progressive optic neuropathy whose main risk factor is intraocular hypertension (IOH). It generates loss of nerves and is the primary cause of irreversible blindness worldwide. The objective of this work was to develop a glaucoma model in rabbits and analyze the anatomical, functional and biochemical changes over time through intraocular pressure (IOP), electroretinography (ERG), antioxidant capacity with FRAP essay. in aqueous humor (AH), and histopathology with quantification of retinal ganglion cells (RGC). 24 female New Zealand white rabbits were used. In 12 animals, glaucoma was induced by injection of ∝-chymotrypsin. During the postoperative period, the treatment and control groups were examined weekly. 7 days after surgery, IOP (mmHg) was 18.30 ± 1.75 in the treatment group and 13.59 ± 0.63 in the control ($p<0.02$). The most important rise was at 14 days (treatment 27 ± 2.64 vs. controls 15.78 ± 0.86) ($p<0.001$), remaining stable thereafter. In the ERG, the analysis of the latency of A and B waves in ms with stimulus intensity of 15 LUX showed a difference between treatment and controls ($p \leq 0.05$). The FRAP values (μM $FeSO_4$/mg of proteins) were 520.3 ± 44 in the treatment group, and 2851.3 ± 178.7 in the control ($p<0.0001$). The RGC count per field was 15 ± 2.20 in the control group and 5.52 ± 0.77 in the treatment group ($p<0.001$). The glaucoma model enabled the analysis of anatomical, functional and biochemical changes as a function of time.

Key words: Glaucoma, Intraocular hypertension, Experimental model, Electroretinography, Total plasma antioxidant capacity.

INTRODUCTION

Glaucoma describes a group of eye disorders with multiple causes, whose common component is progressive optic neuropathy, compromising retinal ganglion cells (RGC), producing their degeneration and death, loss of visual field and blindness. It affects more than 70 million people in the world, causing 10% of bilateral blindness cases, and making this disease the main cause of irreversible blindness (Casson *et al.* 2012).

The mechanism of cell damage that results in a glaucomatous optic neuropathy is not clear, probably because it responds to a complex interaction of multiple agents, including structural and vascular susceptibility. High intraocular pressure (IOP) is an important risk factor for the development of optic neuropathy, and the speed of damage is greater with higher IOP levels (Gupta and Chen 2016).

The mainstay of glaucoma detection, besides tonometry, is examining the optic disk and the retinal cell layer (Yu *et al.* 2016), the anatomical and clinical site where neurodegenerative damage occurs. The typical appearance of glaucomatous optic neuropathy is often

[1]*Cátedra de Física Biomédica. Facultad de Ciencias Médicas. Universidad Nacional de Córdoba. Santa Rosa 1085. (5000) Córdoba, Argentina.*
[2]*Unidad de Investigación y Desarrollo en Tecnología Farmacéutica (UNITEFA-CONICET). Departamento de Ciencias Farmacéuticas, Facultad de Ciencias Químicas, Universidad Nacional de Córdoba, Ciudad Universitaria (5000) Córdoba, Argentina.*
[3] *I Cátedra de Patología. Hospital Nacional de Clínicas. Universidad Nacional de Córdoba. Santa Rosa 1564. (5000) Córdoba, Argentina.*
[4]*Cátedra de Física Biomédica. Carrera de Medicina. Universidad Nacional de La Rioja. De la Fuente S/N. (5300) La Rioja, Argentina.*
**Corresponding author. e- mail: i.tartara@gmail.com*

described as an increase in optic disk excavation, or cupping, produced by a focal or general loss of the retinal neural rim (Mantravadi and Vadhar 2015).

Normally, IOP is regulated by a balance between aqueous humor (AH) discharge and its drainage, either through the trabecular meshwork and Schlemm's canal or the uveoscleral drainage pathway (Jonas *et al.* 2017). The rise in IOP (normal range 11-21 mmHg) is the only known modifiable factor in glaucoma (Mansberger *et al.* 2008). Although the pathogenesis of glaucoma is not fully known, the IOP level is related to the death of RGC (Weinreb *et al.* 2014). Reducing IOP is the only proven treatment of glaucoma so far (Boland *et al.* 2013).

Physical studies have great importance in glaucoma management and the evaluation of its evolution. These include visual field studies and electrophysiological analysis of visual function, such as electroretinography (ERG) (Bach and Poloschek 2013). ERG provides an objective functional test that is easy to obtain in laboratory animals (Rangaswamy *et al.* 2006). By submitting the retina to known light intensities, an electrical response can be obtained and recorded (Mead and Tomarev 2016). The morphology of the ERG response varies with the intensity and duration of the stimulus flash, as well as with the adaptation to light (Wilsey and Fortune 2016).

The existence of glaucoma with normal IOP, the absence of signs of glaucoma in people with elevated IOP, and the progression of neurodegeneration in patients with pharmacologically controlled IOP, made it clear that the factors leading to RGC damage and degeneration are not yet fully defined. Potential contributors are alteration in neurotrophin signaling, oxidative stress, excitotoxicity, mitochondrial dysfunction, incorrect protein folding, hypoxic and ischemic phenomena (Qu *et al.* 2010), and genetic factors (Miller *et al.* 2017). At an ocular level, it has been postulated that oxidative stress promotes chronic glaucoma (Saccà *et al.* 2014) and that antioxidants could protect against glaucoma (Grover and Samson 2014). Determining the molecular biomarkers related to glaucoma may improve clinical tests to diagnose early disease, predict its prognosis, and monitor response to treatment. Hemiretina asymmetry (HA) analysis would be advantageous to obtain specific information in glaucoma (Hondur *et al.* 2017). The ferric reducing antioxidant power (FRAP) assay is a sensitive method used to measure total antioxidant capacity in plasma or serum (Ferreira *et al.* 2004).

Using biological models for experimental research is a valuable tool for understanding the cause and progression of a disease, to explain its pathological processes and develop new therapies (Chew *et al.* 2006). Like many clinical diseases, eye disorders are difficult to investigate in humans due to their physiological and pathological complexity. Although there is no ideal experimental model, biological models aim to reproduce the important aspects of a medical condition so as to understand its mechanisms and develop appropriate treatments (Wormstone and Eldred 2016). Eye disease models in rabbits are very attractive because of their ease of manipulation, short lifespan, low cost, and an anatomical and physiological ocular structure that is comparable to human (Del Amo and Urtti 2015).

In the field of eye pathology research, few specific models are validated for the study of glaucoma, negatively affecting the development of new treatments. The relevance, usefulness and validity of an experimental model must be partially based on its similarity to humans. Given the numerous study methods available for the diagnosis of glaucoma, we consider that histopathological, functional and biochemical analysis of the clinical evolution of the eye in rabbits with induced and sustained ocular hypertension would help to standardize a model of glaucomatous optic neuropathy to evaluate possible new hypotensive and neuroprotective therapies.

The aim of this study was to develop a glaucoma model that allows evaluating new pharmacological treatments.

MATERIALS AND METHODS

Animals

Twenty-four healthy female, non-pregnant, New Zealand White rabbits of 2.5-3 Kg, 3-6 months of age, were used. The animals were not genetically modified. They were given feed and water ad libitum, in a temperature-controlled room (21°C ± 5°C) and exposed to 12 hr. light: 12 hr. dark cycles. To minimize potential confounders the animals were arranged in numbered and individual cages, with environmental enrichment (wooden bar), in the bioterium of the Medical Sciences School (FCM) of the National University of Córdoba (UNC). Before experimentation, the animals remained in their cages for two weeks to acclimatize. In rabbit studies, the number of test animals should be minimized

Table 1. **Average values of A and B waves in control and treatment rabbits at 15 LUX.**

Parameter	Control	Treatment	p Value
A-wave (ms)	26.58	51.825	0.05
B-wave (ms)	49.62	92.4	0.0057
Amplitude (μV)	4.23	3.52	0.4

based on 3R (Reduce, Refine, Replace) principles (Del Amo and Urtti 2015). Appropriate measures were taken to minimize discomfort and pain to the animals. The experiments were carried out following the CICUAL (Institutional Committee for the Care and Use of Laboratory Animals) guidelines (FCM-UNC), in adherence to the National Institute of Health (NIH) Guidelines for the care and use of laboratory animals. The project was approved by CICUAL – FCM – UNC vide No. 44/2017.

Anesthesia and euthanasia

In the induction of glaucoma, aqueous humor extraction, ERG study and eye examinations, general anesthesia was performed with ketamine (3-5mg/Kg) and xylazine (0.5-1mg/Kg). Ocular topical anesthesia was with proparacaine.

After surgery, topical antibiotic therapy was performed with tobramycin and local analgesia with non-steroidal anti-inflammatory drugs (NSAIDs). When measuring IOP, topical anesthesia was used.

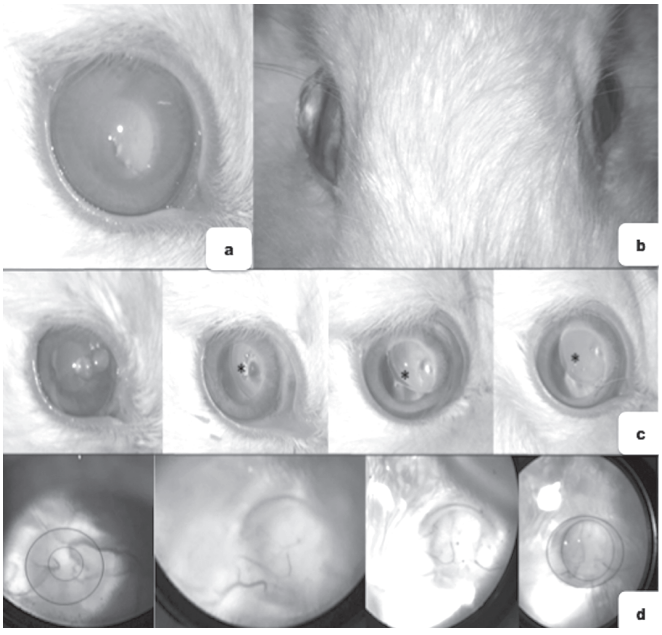

Fig 1. Corneal edema, 7 days after surgery.
[(a) Buftalmos in the right eye of a rabbit 28 days after surgery. (b) Serial photographs of rabbit eye treated. (Days 1, 14, 28 and 42 postoperative). From day 14 the subluxation of the lens (asterisk). (c) is observed. Photographs of ophthalmoscopic examination at 0, 21, 35 and 42 postoperative days photography. (d) shows the difference in the size and deepening of the optic nerve cup, the marked decrease in the neuroretinal ring, and the thinning and eccentric displacement of the retinal vessels. The progressive increase of the optic disk cup is observed from day 0 to day 42 (in the first and last photograph of the optic nerve the edge and the excavation are marked)].

Body temperature, body weight, behavioral changes and pathological changes observed using imaging technology were of criteria that have been used to implement humane endpoints. For euthanasia, the animals were anesthetized as described above, and sacrificed by inhalation of carbon dioxide in a hood.

Groups

The rabbits were divided by group at random and there was no blinding.

a) Controls (without any intervention) (n=12)

b) Treatment (induced glaucoma in the right eye) (n=12).

Glaucoma model

The induction of ocular hypertension was performed in the right eye of the 12 rabbits. A drop of 2% pilocarpine was instilled to cause miosis, then a superior corneal paracentesis was performed, and 0.1 ml of ∝-chymotrypsin (C425-250 mg Sigma Laboratory) at a concentration of 3 mg/ml was injected into the posterior chamber with a 27G cannula (Tártara *et al.* 2017). Three minutes after injection, the anterior chamber was washed with sterile physiological solution. Antibiotics and topical NSAIDs were applied for 7 days. The left eye was not intervened so as not to further affect the welfare of the animal. For the control group, 0.1 ml of a sterile 0.9% sodium chloride solution was injected into the anterior chamber of the right eye.

There was no exclusion of animals during the induction of the experimental model.

Post-surgical evaluation

The follow-up was carried out during 42 days by the following methods.

Eye examination

In 6 ocular hypertensive rabbits after general anesthesia, weekly tests were performed directly for general observation and with a slit lamp for detailed examination of the anterior segment of the eye. To describe the fundus of the eye, a slit lamp with a 90-diopter lens (Volk®) and an indirect binocular ophthalmoscope with a 20-diopter (Volk®) magnifying glass were used. Digital photographs were taken in vivo with a Canon SLR camera mounted on the slit lamp.

IOP measurement was made in twenty animals (10 treated and 10 controls) every 7 days at the same time, under the same environmental conditions and using an iCare® digital manual veterinary tonometer.

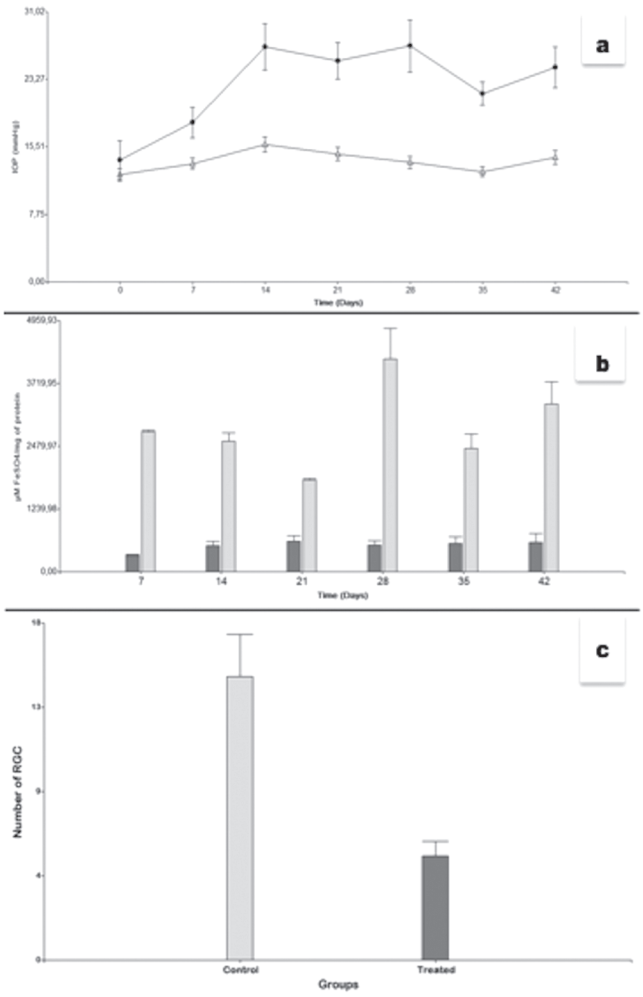

Fig 2a). The mean ± SE of the IOP in mmHg taken weekly is represented.
[The dark circles represent the values of the treated group, and the clear triangles represent the control group ($p < 0.001$). **2b)]. Each bar represents the mean ± SE of µM $FeSO_4$ / mg of proteins in aqueous humor extracted weekly.**
[In dark gray the treated group was represented and in light gray the control. There was a significant difference between the means of both groups on every day ($p < 0.001$). **2c). Each bar represents the mean ± SE of the count of the number of cells per field ($p < 0.001$)].**

Pressure/time curves were made, the mean ± SE of the IOP in mmHg taken weekly is represented. All IOP checks were performed by the same researcher.

Oxidative stress

In four rabbits (2 treated and 2 controls), aqueous humor extraction was carried out weekly to study oxidative stress indicators (200 µL with 30G needles). Samples of the right eyes were obtained in the treatment and control rabbits and preserved at -8°C until processing. Total antioxidant capacity was determined by reduction reaction with iron and tripyridyltriazine.

To determine the total bacterial antioxidant capacity, a method in biological fluids was adapted (Iris and Strain 1999). This technique is based on the reduction of the Fe^{3+}-2,4,6-tris(2-pyridyl)-1,3,5-triazine (TPTZ, SIGMA) complex to its ferrous form, which has an intense blue color that can be monitored at 593 nm. 10 µL of aqueous humor were used and 300 µL of a reagent mixture was added formed by 10 parts of 300 mM acetate buffer with pH 3.6, one part of 10 mM TPTZ (2,4,6-tripyridyl-s-triazine) solution in 40 mM HCl and one of 20 mM ferric chloride solution (FeCl3.6H2O). Aqueous solutions of known concentrations of Fe^{2+} ($FeSO_4.7H_2O$) were used as controls to perform the calibration curve and the final color was determined in a microplate reader (Bio-Rad) at 595 nm. The determination of total proteins was performed with the Bradford method. For this determination, 5 µl of sample was used, to which 250 µl of Bradford reagent was added and read at 595 nm. The results were expressed as µM $FeSO_4$/mg of proteins (Aiassa and Baronetti 2011, Baronetti *et al.* 2013).

Histopathological analysis

Three treatment rabbits and one control rabbit were sacrificed after 45 days of the induction model. The study eye was enucleated, and the material obtained was processed and stained with hematoxylin and eosin. Photographs of 10 fields of the control group and 31 fields of the treatment group were taken, with a 400 X magnification, and the analysis of the retinas was carried out by manual counting of RGC, by two observers independently, using Fiji Image J software®. We consider rabbit retinal ganglion cells to be those located in a linear layer, with large neuronal bodies, large basophilic nuclei and some with evident nucleoli. The non-ganglion cells that make up the ganglion cell layer in the retina of some mammals (amacrines, astrocytes and microglia) have different nuclei, in agreement with the nuclei of the inner nuclear layer. That is, they are smaller, basophils of homogeneous chromatin and are located externally or internally to the ganglion cell line (Muniz *et al.* 2014).

Electroretinography

This was performed in the right eye of two hypertensive rabbits and controls. Before starting, the stimulation threshold was measured in intact rabbits to use as a normal parameter. A flash-type photostimulator was used at an intensity of 11.78 cd.s/m^2 (15 LUX), calibrated manually with a luxometer, with an ambient light of 6.28 cd.s/m^2 (8 LUX). The flash was placed 20 cm from the animal's eye. An AKONIC BIO-PC was used

to amplify and collect the signal. The signal was collected with 100 µV of gain, without attenuation, with filters of high and low frequency (300 Hz - 1.5 Hz) to optimize the measurement. 100 stimuli per study were applied, and the average of the measurements was obtained. To avoid diurnal variations in the responses, the ERGs were performed at the same time of day. Three electrodes were placed in the following way: the reference electrode 0.5 cm from the rear corner of the eye, the active one in contact with the cornea of the studied eye, and the earth electrode on the skull between the ears. The ERGs were analyzed by measuring the latency and amplitude of A and B waves.

Statistical analysis

Statistical t-student tests for paired and independent samples (comparison between different subgroups), as well as non-parametric Man-Whitney and Wilcoxon tests, was used for the comparisons of quantitative variables, when the variables do not meet the normality criteria.

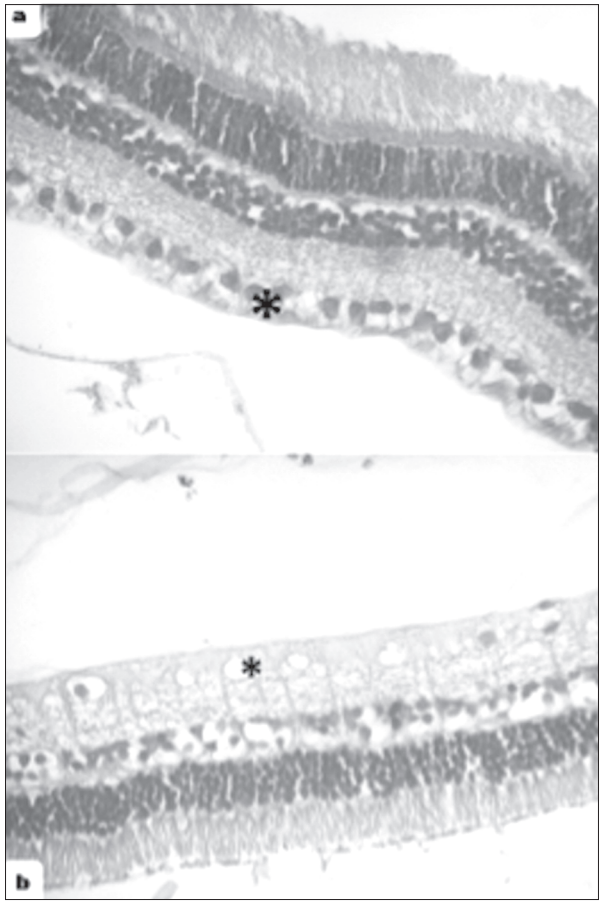

Fig 3a). Photograph of a histological field of control rabbit eye. 3b). Photograph of a histological sample field of rabbit eye operated, 42 days postoperatively. [Asterisks: Layer of ganglion cells of the retina (400X)].

The Irwin-Fisher test will be used for the comparison of proportions. To analyze the relationship between the variables, the Pearson Correlation test will be used, as well as the Multiple Linear Regression analysis (Infostat statistical package Grupo Infostat, Faculty of Agricultural Sciences-National University of Córdoba, Córdoba, Argentina).

RESULTS AND DISCUSSION

Eye examination

In rabbits injected with ∝-chymotrypsin, slight to moderate corneal edema was observed in all treated eye at the immediate post-surgical examination (Fig. 1a), increasing in the first 7 days and then decreasing with time until total transparency of the cornea. At the biomicroscopic ophthalmological examination, the following progressive changes were observed: eye enlargement (buphthalmus) (Fig. 1b), slowing and/or loss of the pupillary reflex, deepening of the anterior chamber, subluxation of the lens (Fig. 1c), and enlargement of the optic disk cup (Fig. 1d). In all control rabbits, no significant changes were observed.

IOP measurement

Figure 2a shows two curves of IOP values expressed in mmHg, one for each group of rabbits (treatment and controls). An increase in IOP values can be observed in the treated group (18.30 ± 1.75) with respect to controls (13.59 ± 0.63) from day 7 ($p < 0.02$), with the greatest increase at 14 days after surgery (27 ± 2.64 vs. 15.78 ± 0.86) ($p < 0.001$), maintaining similar levels during the remaining evaluations (42 days).

Oxidative stress

Figure 2b shows the levels of antioxidant capacity expressed in µM $FeSO_4$ / mg of proteins extracted from aqueous humor in the treatment and control rabbit groups. The level measured in the total days for the treatment group was 520.3 ± 44 and for the controls it was 2851.3 ± 178.7 ($p < 0.0001$).

Histopathological analysis

Figure 2c shows the RGC count per field for control group (n = 10) and treatment (n = 31). In the control group, the number of RGC per field was 15 ± 2.20 and in the treatment group, 5.52 ± 0.77 ($p<0.001$), a 63% decrease. Photographs of fields of eye histological preparations of treatment rabbits and control rabbits can be seen in Fig. 3a, and the decrease in the amount of RGC in the treatment rabbits in Fig. 3b.

Electroretinography

The values obtained in the ERG shown in Table 1, mean latencies observed increased and decreased amplitude in the treated rabbits. Indicative signs of loss of nerve conduction fibers.

The present work aimed to analyze the clinical, histopathological, functional and biochemical evolution of the eye in rabbits with induced and sustained intraocular hypertension (IOH), trying to standardize an experimental model of glaucomatous optic neuropathy, as a starting point for future drug therapies.

Previous studies have developed IOH models in different animal species, such as monkeys, rodents and rabbits (Bouhenni *et al.* 2012). The applicability of these models has been limited by a great variability in IOP and a high incidence of complications. Other glaucoma models were therefore developed, in which attempts were made to damage the ganglion cells of the retina without causing an increase in IOP. Although these were more stable and reproducible, they did not show the natural evolution of the disease.

Our intention was to generate a model of IOH through intraocular injection of ∝-chymotrypsin. Although the technique has been previously described by Lessell and Kuwabara (1969), our work aimed to improve and characterize this technique, reducing postoperative complications and establishing a pattern of anatomical, biochemical and functional deterioration of the model. Standardizing this IOH model would allow it to be used as a basis for investigating future hypotensive and neuroprotective treatments because, as well as lowering the IOP, it was possible to generate progressive deterioration of the optic nerve, characteristic of human glaucoma.

In the model developed by our laboratory, there was a marked increase in IOP until day 14, remaining stable for 42 days after the injection of ∝-chymotrypsin. Using a model of IOP by scleral buckling in rabbits, Wang *et al.* (2019) achieved an increase in IOP immediately after surgery, which peaked 3 hours later (32 ± 3.9 mm Hg) and was consistent for approximately 2 weeks; this IOP value was very similar to that obtained at 14 days in our model. However, Wang's model requires highly specialized surgical skill and specific ophthalmological instruments, which increases its cost Wang *et al.* (2019). A similar situation occurs in the models involving laser to cause fibrosis in the trabecular meshwork (Ishikawa *et al.* 2015). In the course of our experiment, similar maximum IOP values and maintenance time of the IOH were obtained without these requirements, achieving greater ease and lower cost in the procedure.

There are other techniques similar to that which we applied, consisting in the injection of intraocular substances to increase IOP, such as red blood cells, hyaluronic acid, chondroitin sulfate and latex microparticles (Chen and Zhang 2015), which require multiple injections to sustain the IOH, conditioning its stability.

The benefits of the use of the ∝-chymotrypsin injection in our model are the following: it caused a sustained IOH by blocking the trabecular network, decreasing the outflow of aqueous humor (a similar event is observed in chronic human glaucoma); produced buphthalmos (as observed in congenital glaucoma) from the second postoperative week; generated iridian atrophy, loss of pupillary reflexes, and an increase in the cupping of the optic nerve, characteristic of glaucomatous neuropathy. Finally, only a single injection was required.

The rate of evolution of damage *in vivo* observed in our model was greater than that seen in patients with chronic glaucoma, and similar to that of acute glaucoma. This was probably due to the high values of IOP and/or the greater cellular lability of the species (Mantravadi and Vadhar 2015). Therefore, another advantage of this experimental model is that it produces typical characteristics of primary glaucoma.

In other experimental models, loss and/or reduction of RGC was generated by genetic modification, neural excitotoxicity or ischemia-reperfusion methods (Vorwerk *et al.* 1996, Johnson and Tomarev 2010). In spite of achieving changes in the RGC and in the results of ERG, these did not reproduce the clinical symptoms of the disease in humans and showed great variability in IOP changes (Agarwal and Agarwal 2017), which is why they are not very useful for the investigation of hypotensive therapies, although they are useful for the implementation of new neuroprotective treatments (Yoles and Schwartz 1998).

In agreement with other authors, a loss in the amount of RGC was achieved in the model. Gross *et al*., in 2003, measured the amount of RGC in mice with laser photocoagulation-induced glaucoma, and found a percentage decrease of 22.4 ± 7.5 at 4 weeks.

In our laboratory, a 63% decrease in the RGC was found at the end of the sixth week. This demonstrated another advantage of the model developed, since it achieved the neuronal loss of glaucomatous neuropathy. This explains the increase in the cupping of the optic nerve and the alterations of *in vivo* functional tests in the treatment animals. In studies carried out in different species of rodents with induced glaucoma, functional

deterioration was assessed at retina and optic nerve level by means of ERG. A and B waves revealed a significant decrease in their amplitudes between 10 days and 10 weeks (Grozdanic *et al*. 2004, Ben-Shlomo *et al.* 2005, Moreno *et al*. 2005). In our work, by means of an electrophysiological study of previously standardized ERG for rabbits, the functional visual alteration was evaluated *in vivo* in rabbits at an advanced stage of evolution. Significant differences were found between controls and treatment in the values of A and B wave latency at stimulus intensities of 15 LUX, without finding differences between their amplitude. The latter is directly related to the intensity of the light used, and possibly a significant difference in the amplitude of the waves was not found due to limitations in the technique or because of the small number of animals studied. Perhaps the use of higher stimulus intensities could have shown changes in this variable, as explained by Wilsey and Fortune (2016).

No studies have been found that assess ERG in IOP models in rabbits. Bessone *et al.* (2019) generated and evaluated damage in RGC in rabbits without causing IOH, but found no significant differences in the latency and amplitude of A and B waves in ERG, probably because their model at the moment of the analysis did not present the same evolutionary stage as ours.

Although elevated IOP is the most important known risk factor for the development of the disease, there are other factors including ischemia, obstruction of the axoplasmic flow, deprivation of trophic factors, excitoxicity and oxidative stress (Ramdas *et al.* 2018, Kang *et al.* 2003). To analyze the role of oxidative stress in the evolution of the disease, total antioxidant capacity was compared using the FRAP assay in the aqueous humor of treatment and control rabbit eyes. The average antioxidant capacity measured during the 42 postoperative days was 5 times lower than that of controls. The lowest value of FRAP was at 7 days in the treatment rabbits. Ferreira *et al*. (2010) developed a model of glaucoma in rats by cauterization of episcleral veins and measured the total antioxidant capacity in aqueous humor. In agreement with our work, they demonstrated a significant decrease in antioxidant capacity levels in eyes with glaucoma. However, the most evident change was at 30 days after surgery. The difference could be explained by the degree of inflammation generated by the different techniques used to induce the two models, or by the different animal species used.

Hondur *et al*. (2017) performed aqueous humor extraction to measure proteins in patients with glaucoma and compared this with the results in patients without glaucoma. This revealed significantly higher levels of proteins in the AH of glaucoma patients, matching our glaucoma model, in which an increase of total proteins in the AH of treatment rabbits was observed.

CONCLUSION

Our glaucoma model developed and characterized in rabbits allowed us to study the anatomical, functional and biochemical changes as a function of time. The results indicate an important analogy between the model developed and the pathophysiology of glaucoma in humans, which would enable the testing of the efficacy of known or innovative pharmacological therapies.

REFERENCES

Agarwal R, Agarwal P (2017) Rodent models of glaucoma and their applicability for drug discovery. Exper Opin Drug Discov 12(3): 261-270.

Aiassa V, Baronetti JL, Paez PL *et al*. (2011) Increased advanced oxidation of protein products and enhanced total antioxidant capacity in plasma by action of toxins of *Escherichia coli* STEC. Toxicol In Vitro 25(1): 426-431.

Bach M, Poloschek CM (2013) Electrophysiology and glaucoma: current status and future challenges. Cell Tissue Res 353(2): 287-296.

Baronetti JL, Villegas NA, Aiassa V *et al.* (2013) Hemolysin from *Escherichia coli* induces oxidative stress in blood. Toxicon 70: 15-20.

Ben-Shlomo G, Bakalash S, Lambrou GN *et al.* (2005) Pattern electroretinography in a rat model of ocular hypertension: functional evidence for early detection of inner retinal damage. Exp Eye Res 81(3): 340-349.

Bessone CV, Fajreldines HD, Diaz de Barboza GE *et al.* (2019) Protective role of melatonin on retinal ganglionar cell: *In vitro* an *in vivo* evidence. Life Sciences 218: 233-240.

Boland MV, Ervin A-M, Friedman DS *et al*. (2013) Comparative effectiveness of treatments for open-angle glaucoma: a systematic review for the U.S. Preventive Services Task Force. Ann Intern Med 158(4): 271-279.

Bouhenni RA, Dunmire J, Sewell A *et al.* (2012) Animal models of glaucoma. J Biomed Biotechnol 2012: 692-699.

Casson R, Chidlow G, Wood J *et al.* (2012) Definition of glaucoma: clinical and experimental concepts. Clin Exp Ophthalmol 40(4): 341-349.

Chen S, Zhang X (2015) The rodent model of glaucoma and Its implications. Asia Pac J Ophthalmol 4(4): 236-241.

Chew J, Werner L, Stevens S *et al.* (2006) Evaluation of the effects of hydrodissection with antimitotics using a rabbit model of Soemmerings ring formation. Clin Exp Ophthalmol 34(5): 449-456.

Del Amo EM, Urtti A (2015) Rabbit as an animal model for intravitreal pharmacokinetics: Clinical predictability and quality of the published data. Exp Eye Res 137: 111-124.

Ferreira SM, Lerner SF, Brunzini R *et al.* (2004) Oxidative stress markers in aqueous humor of glaucoma patients. Am J Ophthalmol 137(1): 62-69.

Gross RL, Ji J, Chang P, Pennesi ME, Yang Z *et al.* (2003) A mouse model of elevated intraocular pressure: retina and optic nerve findings. Trans Am Ophthalmol Soc 101: 163-169.

Grover AK, Samson SE (2014) Antioxidants and vision health: facts and fiction. Mol Cell Biochem 388(1-2): 173-183.

Grozdanic SD, Kwon YH, Sakaguchi DS *et al.* (2004) Functional evaluation of retina and optic nerve in therat model of chronic ocular hypertension. Exp Eye Res 79(1): 75-83.

Gupta D, Chen PP (2016) Glaucoma. Am Fam Physician 93(8): 668-674.

Hondur G, Gökta^{o} E, Yang X *et al.* (2017) Oxidative stress-related molecular biomarker candidates for glaucoma. Invest Ophthalmol Vis Sci 58(10): 4078-4088.

Iris F, Strain BJ (1999) Ferric reducing/antioxidant power assay: Direct measure of total antioxidant activity of biological fluids and modified version for simultaneous measurement of total antioxidant power and ascorbic acid concentration. Methods in Enzymol 299: 15-27.

Ishikawa M, Yoshitomi T, Zorumski CF *et al.* (2015) Experimentally induced mammalian models of glaucoma. Biomed Res Intern 281214: 1–11. https://doi.org/10.1155/2015/281214.

Johnson TV, Tomarev SI (2010) Rodent models of glaucoma. Brain Res Bull 81(2-3): 349-358.

Jonas JB, Aung T, Bourne RR *et al.* (2017) Glaucoma: Seminar. The Lancet 390: 2183-2193.

Kang JH, Pasquale LR, Willet W *et al.* (2003) Antioxidant intake and primary open angle glaucoma: A prospective study. Am J Epidemiol 158(4): 337-346.

Lessell S, Kuwabara T (1969) Experimental chymotrypsin glaucoma. Arch Ophthal 81(6): 853-864.

Mansberger SL, Medeiros FA, Gordon M (2008) Diagnostic tools for calculation of glaucoma risk. Surv Ophthalmol 53 Suppl 1: S11-S16.

Mantravadi AV, Vadhar N (2015) Glaucoma. Prim Care 42(3): 437-449.

Mead B, Tomarev S (2016) Evaluating retinal ganglion cell loss and dysfunction. Exp Eye Res 151: 96-106.

Miller MA, Fingert JH, Bettis DI (2017) Genetics and genetic testing for glaucoma. Curr Opin Ophthalmol 28(2): 133-138.

Moreno MC, Marcos HJ, Croxatto OJ *et al.* (2005) A new experimental model of glaucoma in rats through intracameral injections of hyaluronic acid. Exp Eye Res 81(1): 71-80.

Muniz JA, de Athaide LM, Gomes BD *et al.* (2014) Ganglion cell and displaced amacrine cell density distribution in the retina of the howler monkey (*Alouatta caraya*). PLoS One 29/9(12): 115291. DOI: 10.1371/journal.pone.0115291.

Qu J, Wang D, Grosskreutz CL (2010) Mechanisms of retinal ganglion cell injury and defense in glaucoma. Exp Eye Res 91(1): 48-53.

Ramdas WD, Schouten JSAG, Webers CAB (2018) The effect of vitamins on glaucoma: A systematic review and meta-analysis. Nutrients 10(3): 359. https://doi.org/10.3390/nu10030359

Rangaswamy NV, Zhou W, Harwerth RS *et al.* (2006) Effect of experimental glaucoma in primates on oscillatory potentials of the slow-sequence mfERG. Invest Opthalmol Vis Sci 47(2): 753-767.

Saccà SC, Pulliero A, Izzotti A (2014) The dysfunction of the trabecular meshwork during glaucoma course. J Cell Physiol 230(3): 510-525.

Tártara LI, Leavi S, Campana V *et al.* (2017) Comparison of two experimental models of glaucoma in rabbits. Rev Fac Cien Med Univ Nac Cordoba 75(1): 25-31.

Vorwerk CK, Lipton SA, Zurakowski D *et al.* (1996) Chronic low-dose glutamate is toxic to retinal ganglion cells: toxicity blocked by memantine. Invest Ophthalmol Vis Sci 37(8): 1618-1624.

Wang Q, Wang J, Lin X *et al.* (2019) Chronic ocular hypertension in rabbits induced by limbal buckling. Br J Ophthalmol 103(1): 144-151.

Weinreb RN, Aung T, Medeiros FA (2014) The pathophysiology and treatment of glaucoma. JAMA 311(18): 1901-1911.

Wilsey LJ, Fortune B (2016) Electroretinography in glaucoma diagnosis. Curr Opin Ophthalmol 27(2): 118-124.

Wormstone IM, Eldred JA (2016) Experimental models for posterior capsule opacification research. Exp Eye Res 142: 2-12.

Yoles E, Schwartz M (1998) Degeneration of spared axons following partial white matter lesion: implications for optic nerve neuropathies. Exp Neurol 153(1): 1-7.

Yu M, Lin C, Weinreb RN *et al.* (2016) Risk of visual field progression in glaucoma patients with progressive retinal nerve fiber layer thinning. Ophthalmol 123(6): 1201-1210.

***Cite this article as:** Caballero GA, Angel-Villegas N, Cremonezzi DC, Campana VR, Palma SD, Allemandi D, Tártara LI (2022) Design and analysis of an efficient glaucoma model for evaluation of pharmacological trials. Explor Anim Med Res 12(1): 109-117. DOI: 10.52635/eamr/ 12.1.109-117.